GA–A23959

# STABILIZATION OF NEOCLASSICAL TEARING MODES BY LOCALIZED ECCD IN DIII–D

by
R. PRATER, R.A. ELLIS, III, R.J. LA HAYE, J.M. LOHR, T.C. LUCE, F.W. PERKINS, C.C. PETTY, J.R. FERRON, D.A. HUMPHREYS, and E.J. STRAIT

MAY 2002

## DISCLAIMER

GA–A23959

# STABILIZATION OF NEOCLASSICAL TEARING MODES BY LOCALIZED ECCD IN DIII–D

by
R. PRATER, R.A. ELLIS, III,† R.J. LA HAYE, J.M. LOHR, T.C. LUCE, F.W. PERKINS,† C.C. PETTY, J.R. FERRON, D.A. HUMPHREYS, and E.J. STRAIT

†Princeton Plasma Physics Laboratory

This is a preprint of a paper presented at the 12th Joint Workshop on Electron Cyclotron Emission and Electron Cyclotron Resonance Heating, May 13–16, 2002, in Aix-en-Provence, France, and to be published in the *Proceedings.*

Work supported by
the U.S. Department of Energy
under Contract Nos. DE-AC03-99ER54463
and DE-AC02-76CH03073

GA PROJECT 30033
MAY 2002

# STABILIZATION OF NEOCLASSICAL TEARING MODES BY LOCALIZED ECCD IN DIII–D

R. PRATER, R.J. LA HAYE, J.M. LOHR, T.C. LUCE, C.C. PETTY, J.R. FERRON, D.A. HUMPHREYS, and E.J. STRAIT

*General Atomics, P.O. Box 85608, San Diego, California 92186-5608*

F.W. PERKINS and R.A. ELLIS, III

*Princeton Plasma Physics Laboratory, P.O. Box 451, Princeton, New Jersey 08543*

Neoclassical tearing modes (NTMs) are MHD modes which can become destabilized in a tokamak by a helical pressure perturbation. The NTM is particularly well suited to control since the mode is linearly stable although nonlinearly unstable, so if the island amplitude can be decreased below a threshold size the mode will decay and vanish. One means of shrinking the island is the replacement of the "missing" bootstrap current by a localized current generated by electron cyclotron current drive (ECCD). This method has been applied to the m=3/n=2 and the 2/1 tearing modes in DIII–D, in H–mode plasmas with ongoing ELMs and sawteeth, both of which generate seed islands periodically. In the case of the 3/2 mode, full suppression was obtained robustly by applying about 1.5 MW of ECCD very near the flux surface of maximum mode amplitude. When the mode first appears in the plasma the stored energy decreases by 30%, but when the mode is stabilized by the ECCD the beta may be raised above the initial threshold pressure by 20% by additional neutral beam heating, thereby effecting an improvement in the limiting beta of nearly a factor 2. An innovative automated search algorithm was implemented to find and retain the optimum location for the ECCD in the presence of the mode. Only partial success has been obtained in stabilizing the 2/1 mode by ECCD, but calculations indicate that ECCD power near 3 MW should be adequate for complete suppression of this mode.

## Introduction

Neoclassical tearing modes (NTMs) are magnetic islands which may grow due to a helically perturbed bootstrap current [1]. The helical loss in bootstrap current is caused by a local reduction of the pressure gradient within the island, since the bootstrap current is generated by radial pressure gradients. The NTM is known to cause significant loss of plasma performance in tokamaks present [2] and planned [3] by limiting the $\beta$ (=plasma pressure/magnetic pressure) which may be attained. For a reactor these limitations may make the difference between economic success and failure [3].

It was pointed out several years ago that the NTM may theoretically be stabilized by the application of a local current drive within the magnetic island to mitigate the reduction of the bootstrap current [4,5]. These authors pointed out that electron cyclotron current drive (ECCD) is a particularly promising approach for this purpose, since ECCD may be highly localized near the intersection of the EC wave with a low order cyclotron resonance. Due to the short wavelength (compared to the antenna size and the plasma gradient scale length), the direction and dispersion of the EC wave bundle may be easily controlled in order to keep the ECCD near the center of the island.

Experiments on the ASDEX-U tokamak first demonstrated the efficacy of this approach [6]. These experiments showed that the amplitude of the m=3/n=2 NTM can be strongly reduced or fully suppressed through the application of ECCD at the optimum radial location. (Here, m is the poloidal mode number and n is the toroidal mode number.) Later experiments on DIII–D also showed that ECCD can completely stabilize the 3/2 NTM [7]. Similar results were obtained on the JT-60U tokamak [8].

The present work advances the state of the art in several ways [9]. First, suppression of the 3/2 NTM in the presence of vigorous sawteeth and ELMs has been demonstrated. This is important because these MHD instabilities are known to trigger the NTMs. Second, we show

that suppression of the 3/2 NTM leads to improved stability, so that the plasma pressure may be increased by at least 60% without instability. Third, several means of determining and maintaining the optimum location of the ECCD, in the presence of shifts of the plasma major radius due to the increase in plasma β, have been successfully tested. And finally, an initial attempt to suppress the faster growing 2/1 NTM has been made.

## Modified Rutherford Equation

The basis of the analysis of the NTM is the well-known modified Rutherford equation [10] for the growth of the island of width w,

$$\frac{\tau_R}{r}\frac{dw}{dt} = \Delta' r + \varepsilon^{1/2}\left(\frac{L_q}{L_p}\right)\beta_p \frac{r}{w}\left[\left(1-\frac{w_{pol}^2}{w^2}\right)-\eta\frac{j_{EC}}{j_{BS}}\right] \quad (1)$$

The first term on the right hand side of Eq. (1) is the classical growth term, which is negative in these experiments; otherwise, the classical tearing mode would grow. The second term becomes positive (tending to growth) when w is sufficiently large, $w > w_{pol}$. Here, $w_{pol}$ represents stabilizing effects which become significant at small island size, like polarization current due to diamagnetic drift, finite perpendicular transport, and finite Larmor radius or drift orbit effects. The last term represents the effects of ECCD. The ratio $j_{EC}/j_{BS}$ is the figure of merit, where $j_{EC}$ is the local current density generated by the ECCD and $j_{BS}$ is the equilibrium bootstrap current. The factor η takes into account the effects of the width $w_{EC}$ of the profile of the ECCD and the offset Δ, of the center of the current drive from the center of the island, and the time behavior (modulated or steady) of the ECCD The driven current is assumed to be Gaussian in shape, $j = j_{EC} \exp[-(r-r_{3/2}-\Delta)^2/w_{EC}^2]$. (In practice on DIII–D the Gaussian approximation is good, with $w_{EC}$ about 1.8 cm, corresponding to $\delta_{EC}$ = 3 cm FWHM).

Equation (1) may be plotted for parameters typical of DIII–D, as shown in Fig. 1. The 3/2 island has a saturation size of about 7.5 cm, determined from measurements of the fluctuations in $T_e$ found from electron cyclotron emission (ECE). Without ECCD the threshold size for growth is around 2 cm, and the growth curve is the top curve in Fig. 1. If ECCD is applied with perfect alignment (Δ=0) with sufficient power that $j_{EC}=j_{BS}$, then the middle curve of Fig. 1 is obtained. The saturated island size is somewhat reduced, from 7.5 cm to 6 cm. If the EC power is increased so that $j_{EC}=2j_{BS}$, then the bottom curve of Fig. 1 is obtained. In this case, the growth rate is negative for any island size and the initially saturated mode amplitude will decrease slowly to about 3 cm and then very rapidly shrink to zero.

Figure 1 also illustrates why the NTM is so suitable to feedback stabilization: it is strongly stable in the limit of small island size, and growth takes place only after a minimum island size has been generated through some other mechanism like sawteeth or ELMs. This implies that the feedback system does not need to address mode amplitudes at the limit of detection, and in theory the feedback power may be turned off between triggers after the mode has been reduced below the threshold size. This has not been demonstrated in practice yet, but it should improve the power economy of a tokamak using current drive to stabilize NTMs.

The factor η in Eq. (1) introduces the effectiveness of the ECCD which is affected by inaccuracy in the location of the applied ECCD and the finite width of the current drive profile. This effect has been studied by Perkins [11] for the case of continuous current drive

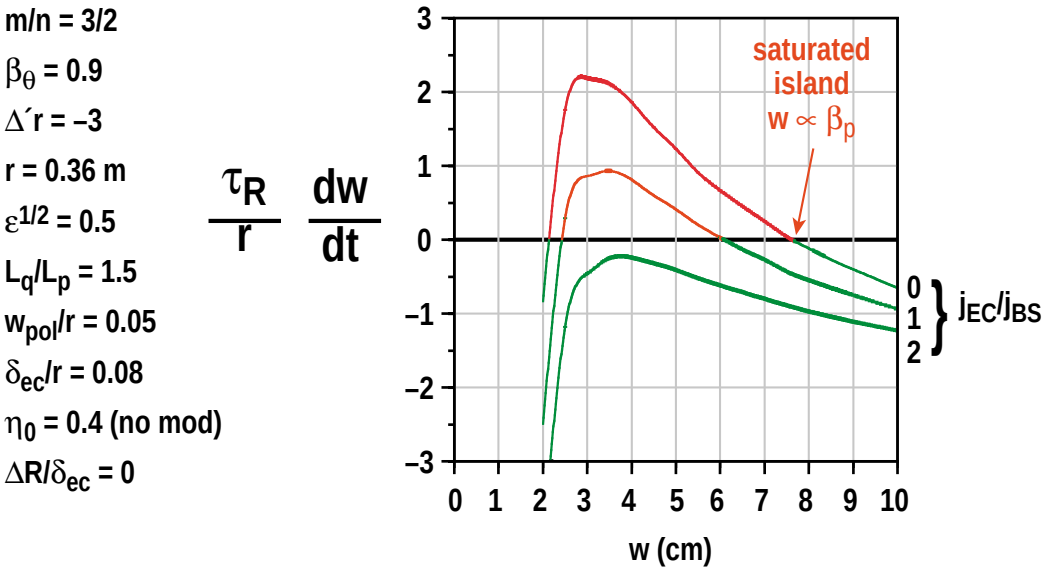


*Fig. 1. Growth rate for the m=3/n=2 island size for different levels of driven current density $j_{EC}$ normalized by the bootstrap current density $j_{BS}$. The growth rate calculation uses parameters typical of DIII–D and assumes perfect alignment of the ECCD and the island.*

and for current drive modulated in phase with the island. For continuous current drive, as applied in these experiments, the efficiency $\eta$ may be plotted as a function of island size normalized to $w_{EC}$ for various values of $\Delta$ as shown in Fig. 2. These curves show the strong sensitivity to $\Delta$ when $w \approx w_{EC}$.

An additional complication is that the current drive applied at the location of the island will modify the equilibrium current profile, changing the classical stability quantity $\Delta'$ in Eq. (1) [12]. In general, the effect is to flatten the current profile and improve the stability. The theory for dealing with both current drive within an island and modification of the equilibrium current profile has not been worked out. This effect is not considered in this paper, but it may be significant.

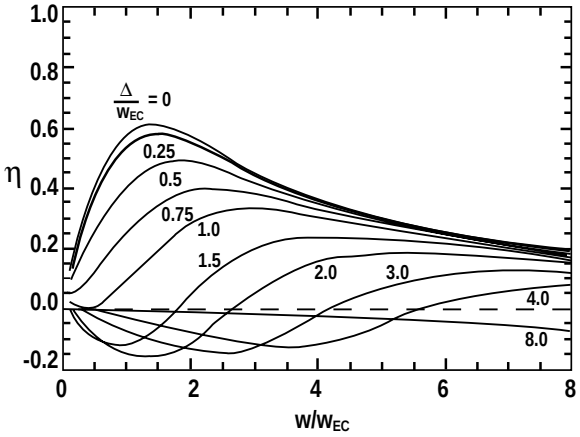


*Fig. 2. Effectiveness $\eta$ of current drive in stabilizing an NTM.*

## Stabilization of the 3/2 NTM by ECCD

Stabilization experiments on DIII–D were carried out using the 110 GHz ECH system [13], using four gyrotrons with power incident on the plasma of about 0.55 MW each. The EC power is directed at the plasma using steerable antennas. The arrangement is shown in Fig. 3. The ECCD is applied near the q=3/2 surface at the inboard midplane in order to minimize electron trapping effects. In Fig. 3, the trajectories of 30 rays from a single antenna are shown. The beam dispersion half angle at half power is 1.7 degrees.

The optimum EC launch conditions were determined for the target equilibrium by running the TORAY-GA code for an array of poloidal and toroidal angles and toroidal fields to find where $j_{EC}$ is maximum. The controlled parameters for the antennas are the facet angle, which is related most closely to the toroidal component of the launched wavevector, and the tilt angle, which is related mostly to the component in the vertical plane. These calculations are shown in Fig. 4, which shows the peak current density and the normalized minor radius $\rho$ of

maximum absorption for a relevant range of angles for the equilibrium shown in Fig. 3. For this case, the q=3/2 surface is near ρ=0.6. Figure 4 shows that the optimum facet angle is near 8 degrees. The calculations show that larger launch angles drive larger total current, but due to the Doppler broadening the peak of the current drive decreases. At smaller launch angles the current drive efficiency decreases too much to compensate for decreased Doppler width, and the peak current density also decreases. For this experiment each antenna was set with a facet near 8 degrees from radial.

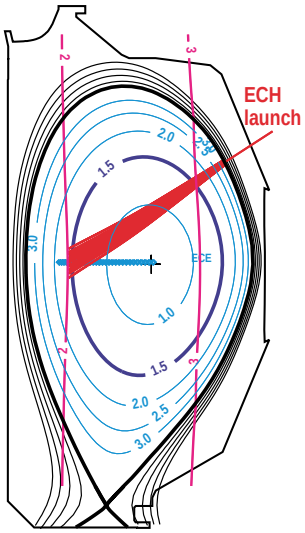


*Fig. 3. Plasma equilibrium, with second and third harmonic electron cyclotron resonances superposed. Also shown is a bundle of 30 rays of equal power simulating the Gaussian beam propagation from a single ECH antenna. The toroidal field is 1.57 T, the plasma current is 1.2 MA, the central electron temperature and density are 2.9 keV and $5\times10^{20}$ $m^{-3}$.*

As discussed in the previous section, the precise location of the ECCD is critical. In order to find the optimum location experimentally, the co-ECCD power was first applied continuously while the magnetic field was slowly ramped down [7]. Since the location of the ECCD is nearly fixed relative to the resonance, which in turn is dependent primarily on the magnitude of the torodial field, this process sweeps the ECCD across the plasma, while the NTM is fixed to the q=3/2 surface which moves much less as the toroidal field decreases. The size of the NTM is followed by determining the amplitude of the n=2 component of the magnetic fluctuations at the vacuum vessel wall through Fourier analysis of a toroidal array of magnetic pickup loops. A typical case is shown in Fig. 5(a). The dip in the n=2 amplitude corresponds to the maximum efficacy of the ECCD. By running the TORAY-GA code for the times just before the dip, at the minimum of the dip, and just after the dip, the expected profile of $j_{EC}$ can be calculated for each case, as shown in Fig. 5(b). This figure shows that the three cases correspond to the minimum distinguishable separation of the current profiles; that is, the space between the peaks is about the same as the width of the peaks. Also shown in Fig. 5(b) is the width of the island as determined from measurements of ECE fluctuations at the frequency of the n=2 magnetic fluctuation, before the ECCD is applied. The alignment of the ECCD with the magnetic island is clearly very sensitive experimentally, in agreement with theory. The bootstrap current density calculated by the ONETWO transport code is also shown in Fig. 5(b). The peak of the ECCD exceeds the bootstrap current density by 30% in this case.

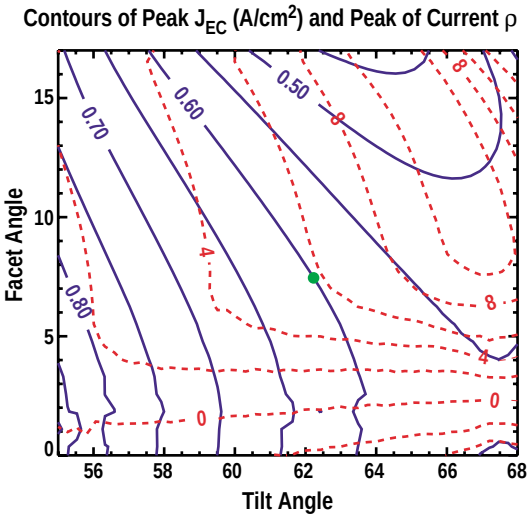


*Fig. 4. The normalized minor radius (solid lines) and the peak ECCD current density (dashed lines, A/cm$^2$), as a function of the launch angles of the ECH antenna, for the equilibrium and geometry of Fig. 2. The tilt angle is related to steering in the vertical direction and the facet angle is related to steering in the toroidal direction. The q=3/2 surface is near ρ=0.6, and the dot shows the parameters used.*

According to the calculation described in the previous section and in Fig. 1, this is approaching the level needed for full stabilization of the mode.

Since alignment of the applied current drive with the location of the island is a central element of the theory, the location of the absorbed EC power was tested by the usual method of modulating the power at 100 Hz and finding the location of the 100 Hz response on the ECE signals [14]. This location can then be compared with the location of the mode using the ECE response at the frequency of the mode, 12.5 kHz [15]. Use of the same ECE channels in both measurements eliminates uncertainty in mapping the heating location to the mode location. Figure 6 shows the good alignment of the location of ECH power deposition with the $T_e$ fluctuations due to the magnetic island for the condition of the middle case of Fig. 5(b).

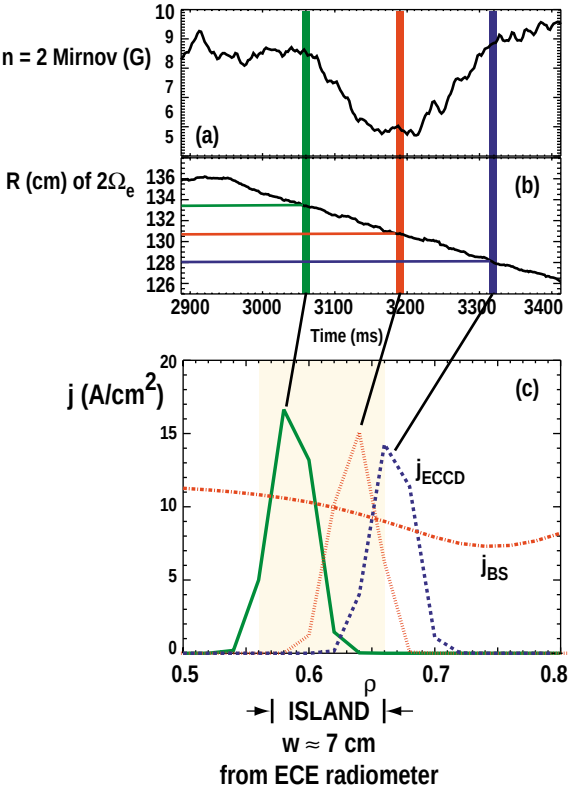


*Fig. 5. (a) n=2 Mirnov amplitude, (b) major radius where the second harmonic of the electron cyclotron frequency matches the applied frequency during a scan of the toroidal field, and (c) calculated ECCD for times corresponding to the arrows for the discharge of Fig. 2.*

When the ECCD is placed in the correct location corresponding to the maximum decrease of the amplitude in Fig. 5, an ECH power of 1.1 MW is sufficient to drive the NTM island size to zero. Figure 7 shows the application of ECCD starting in a discharge with 6 MW of neutral beam heating and with a fully saturated 3/2 NTM present. The effect of the ECCD is to decrease the mode amplitude, and as this happens the normalized beta, $\beta_N$, rises by 35%, where an increase of less than 10% can be attributed to additional heating power added by the ECH system. Hence, confinement is clearly improved by the suppression of the mode. Figure 7(b) also shows that as the n=2 mode decays the amplitude of an n=1 mode grows. This n=1 mode is the sawtooth precursor, and clearly the sawteeth become more vigorous when the n=2 mode has disappeared. Confinement nevertheless improves.

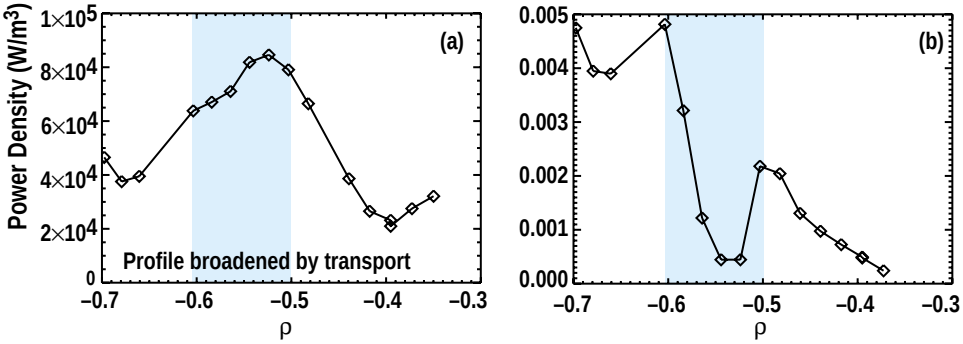


*Fig. 6. (a) Power density inferred from ECE measurements during ECH modulated at 100 Hz versus normalized minor radius, for the conditions of Fig. 2. (b) RMS fluctuation in $T_e$ (keV) measured by ECE at the frequency of the NTM, 12.5 kHz, vs normalized radius. Negative ρ indicates that the measurements are on the high field side of the plasma center.*

The detailed behavior of the mode amplitude after the ECCD is applied can be used to study the physics of the mode suppression. Figure 7(b) shows that the mode amplitude shrinks rapidly at first and then gradually more slowly, until an island size is reached where the decay becomes fast and the mode decreases rapidly into the noise. This knee in the curve at 4 G may be associated with the growth rate of the mode becoming negative and large; that is, w < 3.5 cm for the curve of Fig. 1 with $j_{EC}/j_{BS} = 2$. After the ECH pulse is terminated, the figure shows that the mode growth does not resume, presumably because the n=2 amplitude does not reach the magnitude of the threshold needed for growth in the top curve of Fig. 1.

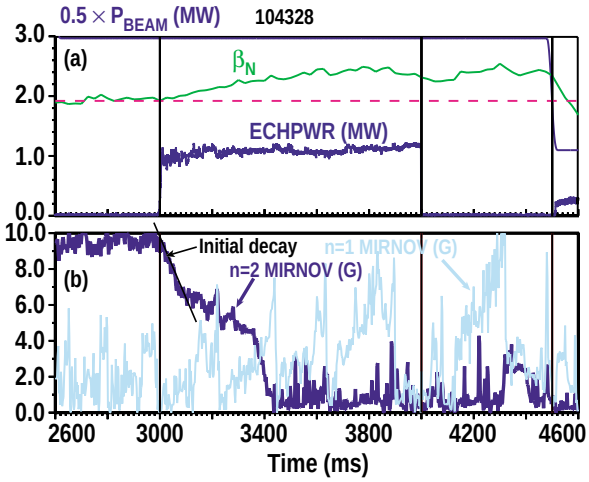


*Fig. 7. (a) $\beta_N$ and ECH power and (b) amplitude of magnetic fluctuations with n=2 (solid line) showing complete suppression of an m/n=3/2 NTM by ECCD and with n=1 (dashed line) showing increased amplitude of the continuing sawteeth, for the same discharge as that of Fig. 2.*

## Increased stability limit when 3/2 NTM is stabilized

The stabilization of the 3/2 NTM has a very practical benefit: the plasma pressure can be increased to well above the previous beta limit. Such a case is shown in Fig. 8. In this discharge the high power phase of the neutral beam heating is started at 1500 ms, and $\beta_N$ rises rapidly to 2.5 in response. This $\beta_N$ is large enough that the 3/2 NTM is destabilized at about 1900 ms, and as this mode grows the $\beta_N$ decreases to 1.7 due to an enhancement of transport caused by the island. At 3000 ms the power from four gyrotrons, 2.2 MW, is added to provide ECCD at the predetermined optimum location on the island center. The NTM amplitude immediately begins to decrease and, as in Fig. 7, it decreases very rapidly to near zero after the island shrinks below a threshold size.

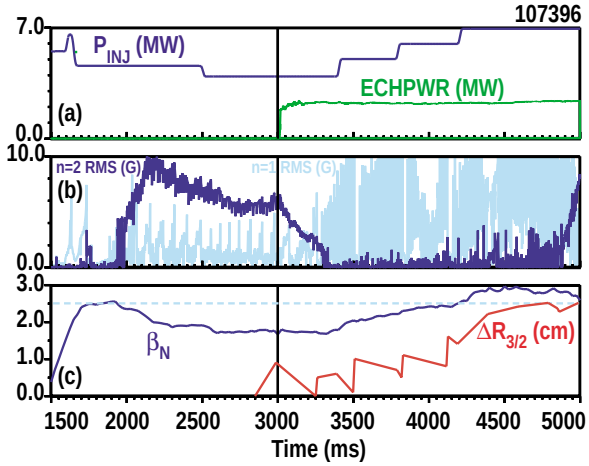


*Fig. 8. Discharge in which the NBI power was raised following suppression of the 3/2 NTM by ECCD. (a) NBI and ECH power, (b) amplitude of n=2 magnetic fluctuations measured by a Mirnov coil array showing full suppression of the NTM, and amplitude of n=1 fluctuations showing increased fishbone activity, and (c) the $\beta_N$ and $\Delta R_{3/2}$, the displacement of the q=3/2 surface at the inboard midplane from its value before the ECH is applied.*

After the amplitude of the 3/2 NTM falls to zero the neutral injection power is increased in preprogrammed steps. The $\beta_N$ increases in response to the greater heating power. At the highest NBI power used, 7 MW, the $\beta_N$ has increased to 3.0, or nearly double the $\beta_N$ when the 3/2 NTM is saturated, and 20% above the $\beta_N$ at which the mode originally started to grow. Since plasma reactivity is proportional to $\beta^2$, these are important advances in the plasma stability.

It can be seen from Fig. 8 that the plasma energy confinement is smaller at 4000 ms, when the ECH is stabilizing the NTM, than at 1750 ms before the mode starts. At least part of this loss of confinement may be attributed to the fishbone instability which arises when the NTM is stabilized. The fishbones are identified as creating the n=1 signal in Fig. 8(b), and the periodic modulation of this signal is due to sawteeth, which also grow in size and decrease in

frequency. Presumably the lower level of MHD activity when the NTM is absent improves the confinement of fast ions from the neutral beam injection. Then the density of fast ions can rise to a large enough level to trigger the fishbones, and fishbones are known to be efficient in transporting fast ions toward the plasma edge.

**Maintaining the optimum location of the ECCD**

It is important that the location of the ECCD retain good alignment with the location of the island. In the discharge of Fig. 8, the 3/2 NTM restrikes at 4850 ms at the crash of a sawtooth. Growth at this sawtooth crash and not at previous crashes is consistent with Eqs. (1–2), since the ECCD is no longer at the optimum position. When the mode is initially stabilized, the plasma center begins moving to larger major radius due to the Shafranov shift associated with the increased beta, while the ECCD location which is anchored primarily to the toroidal field does not. To illustrate this point, the movement of the location of the q=3/2 surface at the inboard midplane, as determined from numerical reconstructions of the equilibrium, from its original position just before the ECH is shown in Fig. 8(c). At the time of the mode growth the displacement has reached 2.5 cm. The FWHM $\delta_{EC}$ of the current drive profile as calculated by the TORAY-GA code is 2.7 cm, and allowing for reasonable relative misalignment of the antennas and enhancement of the EC wave dispersion due to density fluctuations the width is still less than 4 cm. From Fig. 2 with $\Delta=0$ initially shows that the effectiveness of the ECCD in suppressing the NTM at 4850 ms is reduced to less than 30% of its initial value. Hence, the mode may grow when a sawtooth generates a trigger island of sufficient size.

Recognizing that changes to the plasma parameters while the mode is not present can reduce the ability of the ECCD to suppress a mode when a trigger occurs, several strategies have been set up to address this. First, an automated "search and suppress" mechanism has been set up using the digital plasma control system (PCS). In this approach, ECCD is applied at some preset location. If mode growth occurs (as measured by real time analysis of the signals from an array of Mirnov coils), the assumption is that the ECCD is not in the optimum location. Through the PCS, the location of the ECCD is shifted by a small amount and maintained for a brief period. If the mode shrinks but doesn't vanish, another shift in the same direction is produced until the mode either stops shrinking or vanishes. If the mode doesn't shrink, the location is shifted further through a predetermined number of steps, and if no shrinkage occurs the direction is reversed. When the mode vanishes, the location of the ECCD is held fixed. If the initial location is near the optimum location, this process can find the optimum and maintain it through sufficiently small or slow movements of the plasma. Knowledge about which way to move is not required.

Several methods of changing the location of the ECCD are possible, but the applicability of the methods depends on the geometry. If the ECCD is at the inboard midplane, as in Fig. 3, the most effective approach is to have the PCS request a shift of the plasma major radius or of the toroidal magnetic field by a prefixed step corresponding to a change $\Delta R$ of the relative ECCD location by about 1 cm. Both of these approaches have been successfully tested on DIII–D [9]. Figure 9 shows the trajectory of an example discharge in which the toroidal field magnitude was actively shifted to carry out the search for the optimum location. The 3/2 mode is initially saturated, and the PCS carries out a series of shift/dwell steps in $B_T$ corresponding to a displacement of 0.9 cm each, which culminate in the full suppression of the mode. In a comparison discharge, the ECCD is initially applied at the correct location and the mode amplitude decreases monotonically. Discharges in which the initial guess for the direction was wrong have been successfully stabilized by this process. Changing the major radius while keeping $B_T$ fixed works equally well [9].

If the poloidal location of the ECCD on a flux surface lies above the plasma center instead of at the inboard midplane, neither of the two approaches described above are effective in shifting the relative location of the ECCD. For this situation, a plasma shift in the vertical direction is more effective, or the launch angle in the vertical plane of the EC waves may be changed. These techniques will be tested in the future. In any case, the "blind search" used in this work may be improved by obtaining real time estimates of the magnitude and direction of the optimum step size. This is being carried out on DIII–D through use of real time equilibrium reconstructions as part of the PCS.

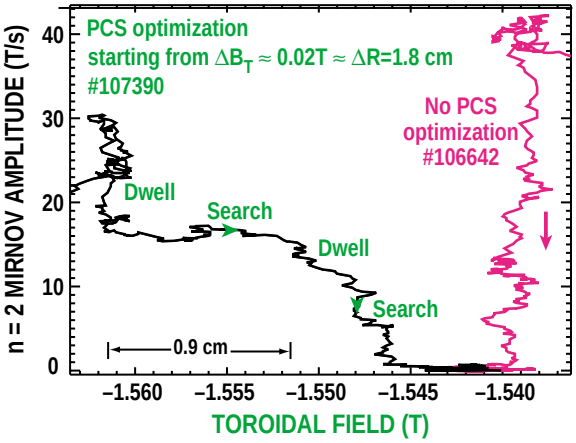


*Fig. 9. Trajectory of the amplitude of the n=2 magnetic perturbation (related to the size of the magnetic island) versus toroidal field, for two discharges. In one the toroidal field is initially at a value which places the ECCD at a non-optimum location, and the PCS carries out a "search and suppress" process which varies $B_T$ and results in full stabilization. In the other discharge the ECCD is initially at the correct location and the mode amplitude drops to zero.*

## Conclusions

Localized ECCD applied in the optimum location has proved to be a reliable and robust means of fully suppressing the 3/2 NTM [9], in validation of theoretical predictions which originated before experiments were attempted [4,5]. When the NTM is stabilized the plasma beta rises more than expected from the additional heating power of the ECH, and when further beam heating is added the beta can be raised to as high as 60% above the beta when the saturated mode is present. Several means of keeping the ECCD at the appropriate location through a seeking process of small shifts of the plasma location or the toroidal field have been used successfully.

## Acknowledgment

Work supported by U.S. Department of Energy under Contracts DE-AC03-99ER54463 and DE-AC02-76CH03073.

## References

[1] Z. Chang, et al., Phys. Rev. Letters **74**, 4663 (1995).
[2] R. J. La Haye, et al., Phys. Plasmas **7**, 3349 (2000).
[3] ITER Physics Basis Editors, et al., Nucl. Fusion **39**, 2137 (1999).
[4] C.C. Hegna and J.D. Callen, Phys. Plasmas **4**, 2940 (1997).
[5] H. Zohm, Phys. Plasmas **4**, 3433 (1997).
[6] G. Gantenbein, et al., Phys. Rev. Letters **85**, 1242 (2000).
[7] R. Prater, et al., in Fusion Energy 2000, 18th Conferenece Proceedings, Sorrento, Italy 2000 (IAEA, Vienna, 2001), paper EX8/1.
[8] A. Isayama, et al., Plasma Phys. Cont. Fusion **42**, 137 (2001).
[9] R.J. La Haye, et al., "Control of Neoclassical Tearing Modes in DIII–D," to be published in Phys. Plasmas.
[10] R.J. La Haye, et al., Madeiras EPS.
[11] F.W. Perkins et al., Proceedings of the 24th European Physical Society Conference on Controlled Fusion and Plasma Physics (EPS, Petit Lancy, 1997), Part III p. 1017.
[12] A. Pletzer and F.W. Perkins, Phys. Plasmas **6**, 1589 (1999).
[13] J. Lohr, ECH system.
[14] C.C. Petty, et al., in Radio Frequency Power in Plasmas, 13th Topical Conference, Annapolis, Maryland 1999 (AIP, Melville, NY, 1999), p. 245.
[15] T.C. Luce, et al., in Radio Frequency Power in Plasmas, 14th Topical Conference, Oxnard, California 2001 (AIP, Melville, NY, 2001), p. 306.